Structure and Successive Phase Transitions of $RGeBr_3$ (R = Alkylammonium) Studied by Means of NQR *

Tsutomu Okuda [1], Shusaku Gotou [1], Toshirou Takahashi [1], Hiromitsu Terao [2], and Koji Yamada [1]

[1] Department of Chemistry, Faculty of Science, Hiroshima University, Kagamiyama 1 Chome, Higashi-Hiroshima 739, Japan
[2] Faculty of Integrated Arts and Sciences, Tokushima University, Minamijosanjima-cho, Tokushima 770, Japan

Z. Naturforsch. **51a,** 686–692 (1996); received October 10, 1995

A series of tribromogermanate(II) complexes $RGeBr_3$ ($R = CH_3NH_3$, $(CH_3)_2NH_2$, $(CH_3)_4N$, $C_2H_5NH_3$, $(C_2H_5)_4N$) have been synthesized and characterized by ^{81}Br NQR, AC conductivity, DTA, and X-rax diffraction. These measurements revealed the presence of successive phase transitions in these complexes. The crystal structures of Phases I and II in $(NH_3)_4NGeBr_3$ were derived from the Rietveld analysis of powder X-ray diffraction. The electric conductivity was considerably high in $CH_3NH_3GeBr_3$ and $(NH_3)_4NGeBr_3$. The conduction mechanism is discussed on the basis of ^{81}Br NQR spin-lattice relaxation times and crystal structures.

Key words: ^{81}Br NQR, T_1, Phase Transition, Ionic Motion, Ionic Conductivity.

Introduction

The MX_3^- (M = Group 14 elements, X = halogen) ions have various shapes such as trigonal pyramid, square pyramid, and octahedron depending on the formation of halogen bridges. These complexes are expected to undergo phase transitions by cationic and anionic motions excited with increasing temperature. For alkylammonium trichlorogermanate(II) complexes, we have already reported that their ionic conductivity increased abruptly at the phase transition point, and the mobile ion was confirmed to be the chloride ion by means of ^{35}Cl NQR and X-ray diffraction [1, 2].

In the present study, several tribromogermanate(II) complexes were synthesized and the ionic motions and successive phase transitions were examined by measuring ^{81}Br NQR, X-ray diffraction, DTA, and electric conductivity in order to clarify the conduction mechanism in these systems.

Experimental

$RGeBr_3$ ($R = CH_3NH_3$, $(CH_3)_2NH_2$, $(CH_3)_4N$, $C_2H_5NH_3$, $(C_2H_5)_4N$) were prepared as follows: (a) $Ge(OH)_2$ was prepared from GeO_2 by the method described in [3]. (b) the solution obtained by dissolving $Ge(OH)_2$ into concentrated hydrobromic acid was held in a water bath at 80 °C for 30 minutes and then added to a stoichiometric amount of alkylammonium bromide obtained by dissolving alkylamine in concentrated hydrobromic acid. The complexes thus obtained were identified by CHN elemental analysis as listed in Table 1. In the case of $(CH_3)_4NGeBr_3$, the sample was identified by the Rietveld analysis of the powder X-ray diffraction pattern.

Table 1. Chemical analysis of tribromogermanate(II) complexes.

Compound	Found (%)			Calculated (%)		
	C	H	N	C	H	N
$CH_3NH_3GeBr_3$	3.41	1.63	3.94	3.48	1.76	4.07
$(CH_3)_2NH_2GeBr_3$	7.24	2.51	4.09	6.70	2.25	3.91
$C_2H_5NH_3GeBr_3$	6.54	2.29	4.36	6.72	1.97	3.92
$(C_2H_5)_4NGeBr_3$	21.43	4.61	3.24	21.70	4.52	3.16

---

* Presented at the XIIIth International Symposium on Nuclear Quadrupole Interactions, Providence, Rhode Island, USA, July 23–28, 1995.

Reprint requests to Prof. T. Okuda.

0932-0784 / 96 / 0500-0686 $ 06.00 © – Verlag der Zeitschrift für Naturforschung, D-72072 Tübingen

Table 2. Crystal data and experimental details of the Rietveld analysis for $CH_3NH_3GeBr_3$ and $(CH_3)_4NGeBr_3$.

Compound	$CH_3NH_3GeBr_3$	$(CH_3)_4NGeBr_3$	
Phase	I	I	II
Temperature/K	297	453	297
Crystal system	Rhombohedral	Cubic	Orthorhombic
Space group	R3m	Pm3m	Pnma
Lattice constant	$a = 5.815(1)$ Å $\alpha = 88.58(1)$ °	$a = 6.769(1)$ Å	$a = 13.334(1)$ Å $b = 9.444(1)$ Å $c = 9.211(1)$ Å
Z	1	4	1
d_{cal}/g cm^{-3}	2.97	2.186	2.337
Number of parameters	29	23	33
2θ range/Degree	10–60	10–60	10–60
Step width/Degree	0.02	0.02	0.02
R_F,[a] R_p [b]	0.059, 0.070	0.062, 0.128	0.065, 0.048
DS/°, RS/mm, SS/° [c]	0.5, 0.15, 0.5	0.5, 0.15, 0.5	0.5, 0.15, 0.5

[a] $R_F = \Sigma |(I_K(\mathrm{obs}))^{1/2} - (I_K(\mathrm{cal}))^{1/2}| \Sigma I_K(\mathrm{obs})^{1/2}$, where I_K is the intensity assigned to the Kth Bragg reflection.
[b] $R_p = \Sigma |y_i(\mathrm{obs}) - y_i(\mathrm{cal})| / \Sigma y_i(\mathrm{obs})$, where $y_i(\mathrm{obs})$ and $y_i(\mathrm{cal})$ are the observed and calculated intensity at the ith step.
[c] Divergence slit, receiving slit, and scatter slit.

^{81}Br NQR signals were observed by a Matec pulsed spectrometer. The spin-lattice relaxation times of NQR were determined by a conventional pulse technique.

The temperature dependence of the ionic conductivity was measured by means of a complex impedance method [1].

The X-ray powder diffraction patterns were obtained by using a Rigaku Rad-B system, and the observed diffraction patterns were analysed by the Rietveld method, the computing program of which was developed by Izumi [4]. The experimental details on the Rietveld analysis are summarized in Table 2 together with crystallographic data.

Results and Discussion

Figure 1 shows the phases and phase transition temperatures in tribromogermanate(II) complexes. They were mainly determined by DTA. Since the phase transitions at about 400 K in $CH_3NH_3GeBr_3$ and at 237 K in $(CH_3)_4NGeBr_3$ could not be detected by DTA, the former transition was determined by X-ray diffraction and the latter by NQR. In the DTA curves of $(C_2H_5)_4NGeBr_3$, three endothermic peaks appeared at 323, 336, and 372 K on heating, while three exothermic ones appeared at 365, 325, and 294 K on cooling. The anomaly at the highest temperature is melting. Since the middle peak was large and the lower two peaks were close to each other, definite transition temperatures could not be determined. The middle peak was apparently larger than the melting peak, and the enthalpy of transition is larger than the enthalpy of melting, suggesting the presence of a plastic crystalline phase.

There exist no available crystal structural data for the present complexes though Thiele et al. have reported the crystal structure of $RbGeBr_3$ obtained from single crystal X-ray diffraction [5]. In order to obtain information about the anionic structure, we measured the powder X-ray diffraction and analysed its pattern by the Rietveld method. The final parameters are listed in Table 3. Figures 2 and 3 show the powder X-ray diffraction pattern and the crystal structures of Phases I and II in $(CH_3)_4NGeBr_3$. Although their fundamental structure is perovskitic, the crystal structure changes from cubic to a less symmetric system depending on the symmetry of the Br-Ge-Br bond in the crystal. The cubic system has an infinite chain formed by the complex anions where the

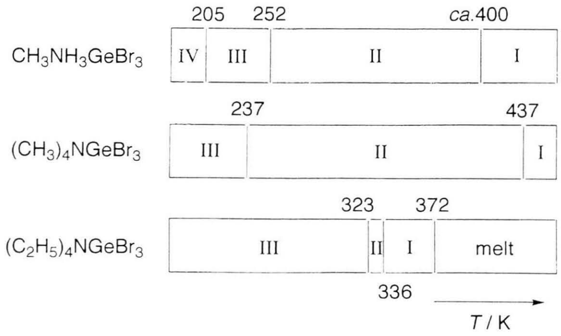

Fig. 1. Phase transitions of tribromogermanate(II) complexes.

Table 3. Positional and isotropic thermal parameters of $CH_3NH_3GeBr_3$ and $(CH_3)_4NGeBr_3$

Compound	Atom	Position[a]	x	y	z	$B_{iso}/Å^2$
$CH_3NH_3GeBr_3$	CH_3NH_3[b]	1a (3m)	0.0	0.0	0.0	35 (7)
	Ge	1a (3a)	0.47 (2)	0.47 (2)	0.47 (2)	2 (1)
	Br	3b (m)	0.49 (2)	0.49 (2)	0.03 (2)	8 (4)
$(CH_3)_4NGeBr_3$	$(CH_3)_4N$[c]	1a (m3m)	0.0	0.0	0.0	81 (6)
(Phase I)	Ge	1b (m3m)	0.5	0.5	0.5	21 (4)
	Br	6f (4mm)	0.129 (4)	0.5	0.5	17 (4)
$(CH_3)_4NGeBr_3$	$(CH_3)_4N$[c]	4c (m)	0.508 (3)	0.25	0.236 (5)	72 (2)
(Phase II)	Ge	4c (m)	0.759 (1)	0.25	0.746 (2)	5.8 (6)
	Br (1)	8d (1)	0.757 (1)	0.055 (1)	0.568 (1)	6.9 (5)
	Br (2)	4c (m)	0.941 (1)	0.25	0.795 (2)	7.5 (7)

[a] Wykoff notation and point symmetry.
[b] The isoelectronic dummy atom K^+ was used for the refinement.
[c] The isoelectronic dummy atom Mo was used for the refinement.

Ge atom is coordinated by six Br atoms and the lower symmetric system has a discrete $GeBr_3^-$ anion. The cubic system is also formed as a results of an averaged structure of the disordered state at the higher temperatures [1, 2]. It becomes apparent from Fig. 3 that the disorder of the Br sites in Phase I leads to the more symmetric cubic crystal. Such a structural change is also expected to occur in $(C_2H_5)_4NGeBr_3$, Phase I of which yielded weak diffraction peaks assigned to the cubic phase.

^{81}Br NQR was observed for these complexes. $(C_2H_5)_4NGeBr_3$ showed complicated spectra as shown in Figure 4. This spectrum was taken point by point changing the frequency, and the echo intensity was plotted. Since each resonance line was broad at least six large peaks were apparently recognized. Their frequencies are listed in Table 4 suggesting the presence of at least two nonequivalent $GeBr_3^-$ anions. As the number of alkyl groups increases, the mean NQR frequencies increases considerably as seen from Table 4, suggesting that the interaction of the Br atom

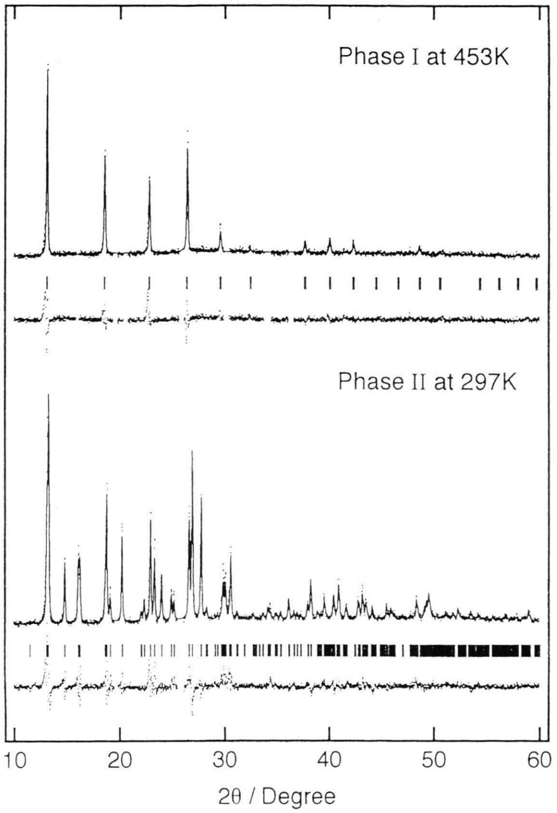

Fig. 2. X-ray diffraction patterns of Phase I and Phase II in $(CH_3)_4NGeBr_3$. The calculated and observed patterns are shown by solid-lines and dots, respectively. The lower portion is a plot of the difference between them. The vertical marks below the patterns indicate the position of the reflections included in the calculations.

Table 4. ^{81}Br NQR frequencies in tribromogermanate(II) complexes at 77 K.

Compound	Frequency MHz			Mean frequency MHz
$CH_3NH_3GeBr_3$	84.58,	86.17,	87.89	86.21
$(CH_3)_2NH_2GeBr_3$	89.36,	92.60,	94.80	92.25
$(CH_3)_4NGeBr_3$	95.009	96.740	96.880	96.210
$C_2H_5NH_3GeBr_3$	76.741,	79.821,	84.191	80.251
$(C_2H_5)_4NGeBr_3$	91.6,	93.1,	94.3,	94.8
	96.2,	96.7,	97.0	

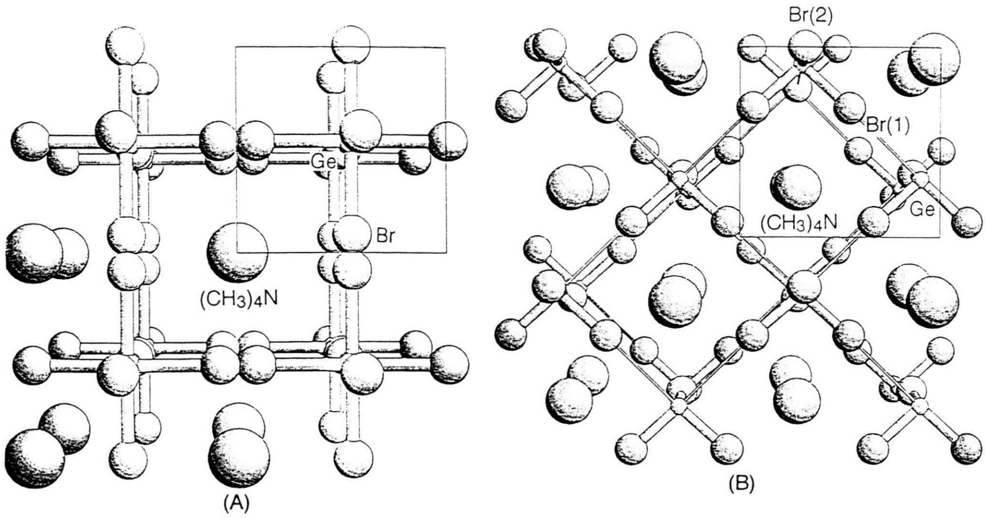

Fig. 3. Crystal structures of (A) Phase I and (B) Phase II in $(CH_3)_4NGeBr_3$.

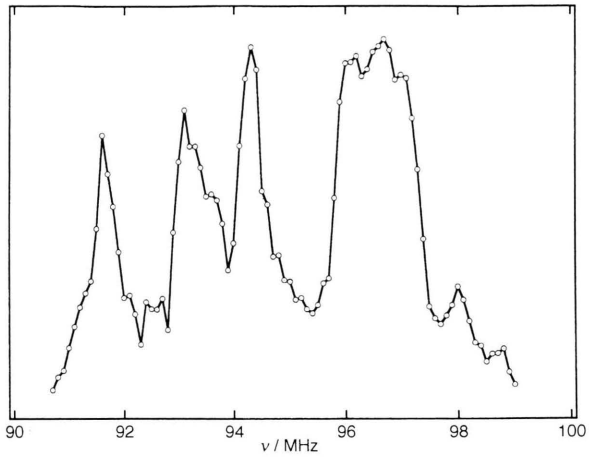

Fig. 4. Echo plot of ^{81}Br NQR in $(C_2H_5)_4NGeBr_3$.

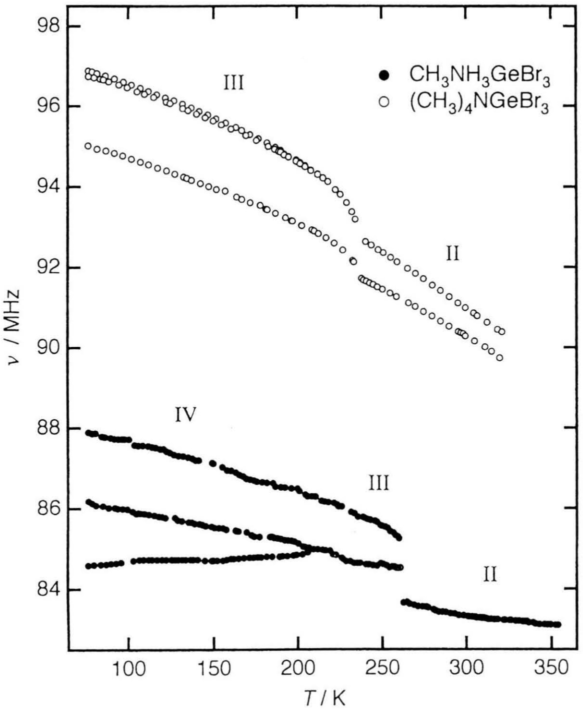

Fig. 5. Temperature dependence of ^{81}Br NQR frequencies in $CH_3NH_3GeBr_3$ and $(CH_3)_4NGeBr_3$.

with cations becomes weaker with increasing the number of alkyl groups because of a decrease in the number of H atoms bonded to the N atom.

Figure 5 shows the temperature dependence of the ^{81}Br NQR frequencies in $CH_3NH_3GeBr_3$ and $(CH_3)_4NGeBr_3$. When the temperature was increased from 77 K in $CH_3NH_3GeBr_3$, two lower resonance lines coalesced at 205 K, and only one resonance line was observed above 260 K. With a further increase in temperature, the resonance line disappeared at 355 K.

On the other hand, with increasing temperature from 77 K in $(CH_3)_4NGeBr_3$, three resonance lines decreased their frequencies and the higher two lines coalesced at 236 K, indicating the presence of a second order phase transition. With a further increase in temperature, all lines disappeared at 320 K.

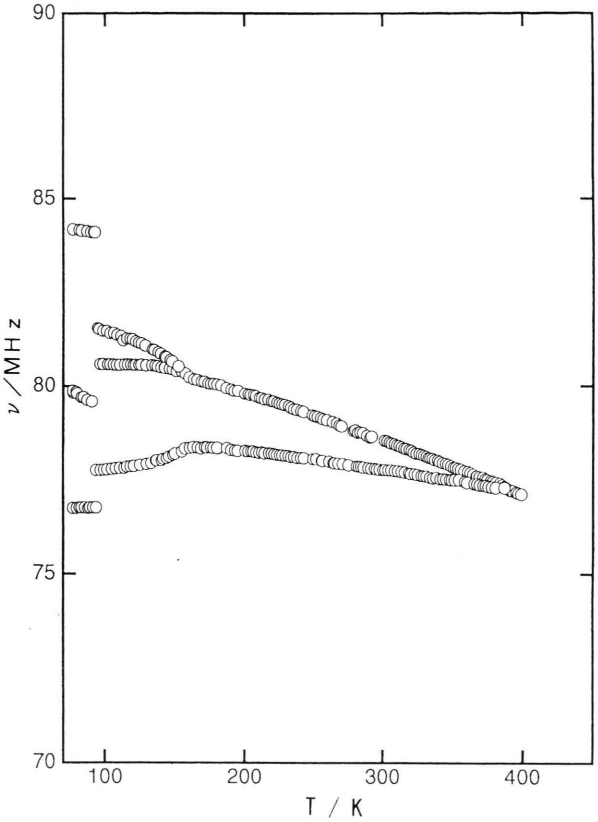

Fig. 6. Temperature dependence of ^{81}Br NQR frequencies in $C_2H_5NH_3GeBr_3$.

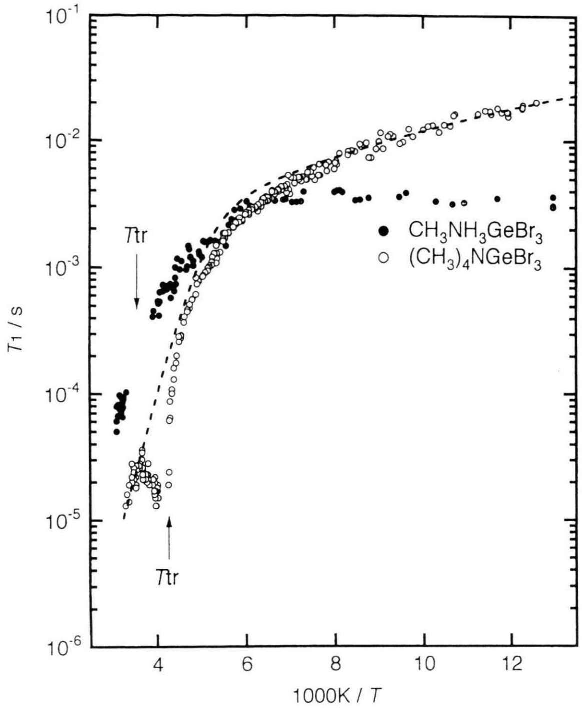

Fig. 7. Temperature dependence of ^{81}Br NQR spin-lattice relaxation time in $CH_3NH_3GeBr_3$ and $(CH_3)_4NGeBr_3$.

Figure 6 shows the temperature dependence of the ^{81}Br NQR frequencies in $C_2H_5NH_3GeBr_3$. Three ^{81}Br resonance lines were observed at 77 K. When the temperature was increased, these frequencies changed discontinuously at 93 K. When the temperature reached 170 K, one pair of them coalesced and the rest changed its slope. With a further increase in temperature, two lines coalesced at 390 K. These findings suggest that the phase transition at 93 K is first order and the remaining ones are second order. These transition temperatures are in good agreement with those obtained from DTA.

In order to obtain information on the motion of the anion, we observed the ^{81}Br NQR spin-lattice relaxation time (T_1) for these complexes. Figure 7 shows the results for $CH_3NH_3GeBr_3$ and $(CH_3)_4NGeBr_3$. At 77 to 150 K, T_1 for $CH_3NH_3GeBr_3$ is almost constant, indicating the presence of an other relaxation mechanism except lattice vibrations and then decreased exponentially above 150 K. As for $(CH_3)_4NGeBr_3$, T_1 decreased gradually with increasing temperature owing to lattice vibrations. When the temperature was further increased, a sharp dip due to a phase transition occurred at about 190 K, and then a rapid decrease began from about 290 K.

The disappearance of the resonance line, did show that the $GeBr_3$ anion began to reorient around its three-fold symmetry axis at about 150 K. In general, T_1 is the sum of contributions from the lattice vibration of the ions and the reorientation of the anion, when each motion is assumed to be independent [6, 7].

$$1/(T_1)_{\text{obs}} = 1/(T_1)_{\text{lat}} + 1/(T_1)_{\text{reo}}\,, \tag{1}$$

$$1/(T_1)_{\text{lat}} \;= a\,T^n\,,$$

$$1/(T_1)_{\text{reo}} \;= b\,\exp(-E_a/R\,T)\,,$$

where E_a is the activation energy of the motion. By fitting (1) to the experimental T_1 values, we obtained for $(CH_3)_4NGeBr_3$

$$1/(T_1)_{\text{obs}} = 3.03\times10^{-3}\times T^{2.22} + 1.66\times10^{9}\exp(-25.0/R\,T)\,.$$

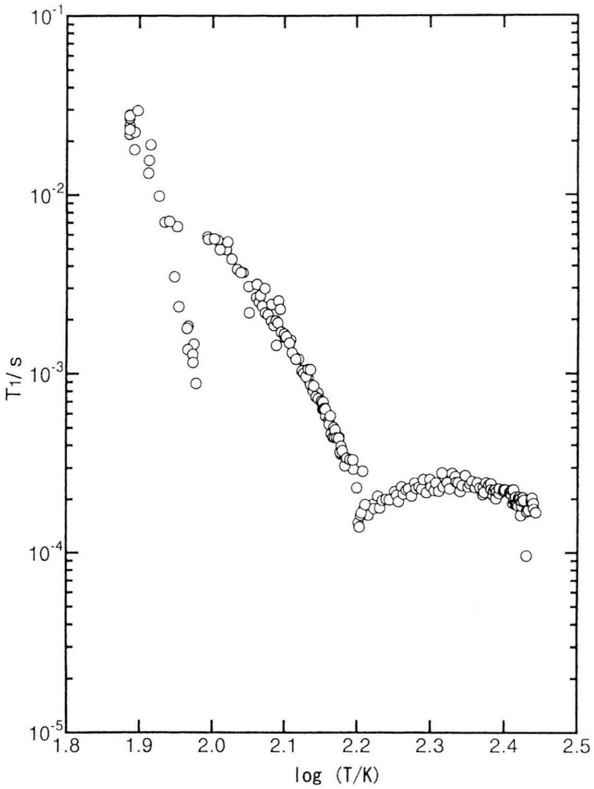

Fig. 8. Temperature dependence of ^{81}Br NQR spin-lattice relaxation time in $C_2H_5NH_3GeBr_3$.

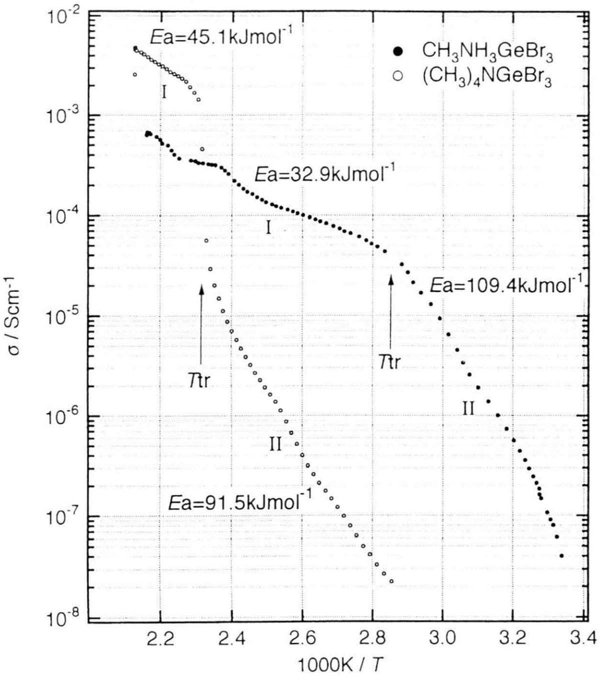

Fig. 9. Temperature dependence of the AC conductivity of $(CH_3)_4NGeBr_3$.

For $CH_3NH_3GeBr_3$, the activation energy of reorientation of the anion was obtained to be 35 kJ/mol from the slope of the curve in the high temperature range. These values are too small compared to those of the trichlorogermanate(II) complexes [1]. One of the causes is that, since there is a phase transition in the temperature range where T_1 decreased rapidly, the activation energy could bot be obtained accurately.

Figure 8 shows the temperature dependence of the ^{81}Br NQR spin-lattice relaxation time in $C_2H_5NH_3GeBr_3$. There is a sharp dip near 95 K and a small dip near 160 K, suggesting critical fluctuations of the anionic motion near the phase transition. The transition points are in good agreement with those from the NQR frequency measurements. Both experimental results indicate that the transitions near 95 K and 160 K are of first and second order, respectively.

Figure 9 shows the temperature dependence of the AC conductivity in $CH_3NH_3GeBr_3$ and $(CH_3)_4NGeBr_3$. Their conductivities are almost equal but smaller by two orders of magnitude than those of the corresponding chlorides. For $CH_3NH_3GeBr_3$, the conductivity decreased gradually with decreasing temperature, and at about 340 K the slope of the curve changed significantly. The conductivity of $(CH_3)_4NGeBr_3$ decreased monotonously with decreasing temperature, and the slope changed more sharply at the phase transition point. We evaluated activation energies from the linear portion of the $\ln \sigma$ vs. $1/T$ graphs using the Arrhenius equation

$$\sigma = \sigma_0 \exp(-E_a/R\,T). \qquad (2)$$

The results are 32.9 kJ/mol and 109.4 kJ/mol for Phase I and Phase II of $CH_3NH_3GeBr_3$, and 45.1 kJ/mol and 91.5 kJ/mol for Phase I and Phase II of $(CH_3)_4NGeBr_3$. These values in Phase I are comparable with those in Phase I of the corresponding chlorides, suggesting a disordered structure [1].

As to the high ionic conductivity, there are two possible mechanisms, (a) self diffusion of cations and (b) jumps of Br$^-$ and reorientation of $GeBr_3^-$ [1]. For $CH_3NH_3GeBr_3$ and $(CH_3)_4NGeBr_3$, the latter mechanism seems prevail because the ^{1}H NMR of Phase I in both complexes did not show a sharp line width due to self diffusion of cations, T_1 of ^{81}Br NQR supported the occurrence of reorientation of $GeBr_3^-$ anion at the high temperature phase, and the crystal structure from X-ray diffraction showed disorder of bromide atoms in Phase I of $(CH_3)_4NGeBr_3$.

Acknowledgement

This work was supported by the Grant-in-Aid for Scientific Research on Priority Area of "Solid State Ionics", (Area No. 260/07239237) from the Ministry of Education, Science and Culture, Japan.

[1] K. Yamada, K. Isobe, T. Okuda, and Y. Furukawa, Z. Naturforsch. **49a,** 258 (1994).
[2] K. Yamada, K. Isobe, E. Tsuyama, T. Okuda, and Y. Furukawa, Solid State Ionics **79,** 152 (1995).
[3] W. C. Fernelius, Inorganic Syntheses, Vol. 2, McGraw-Hill, New York 1946, pp. 102–105.
[4] F. Izumi, The Rietveld Method, ed. by R. A. Young, Oxford Univ. Press, Oxford 1993.
[5] G. Thiele, H. W. Rotter, and K. D. Schmidt, Z. Anorg. Allg. Chem. **559,** 7 (1988).
[6] N. E. Ainbinder and I. G. Shaposhnikov, Advances in Nuclear Quadrupole Resonance, Vol. 3, ed. by J. A. S. Smith, Heyden & Son Ltd., London 1978, p. 122.
[7] H. Chihara and N. Nakamura, Advances in Nuclear Quadrupole Resonance, Vol. 4, ed. by J. A. S. Smith, Heyden & Son Ltd., London 1980, p. 37.